

3 Bo Hu^{1,*}, Sara Lelek^{2,3,*,**}, Bastiaan Spanjaard^{1,*,**}, Mariana Guedes Simões², Hananeh
4 Aliee⁴, Ronny Schäfer¹, Fabian Theis⁴, Daniela Panáková^{2,3,***}, Jan Philipp Junker^{1,***}

6 ¹Berlin Institute for Medical Systems Biology, Max Delbrück Center for Molecular Medicine, Berlin,
7 Germany

8 ² Max Delbrück Center for Molecular Medicine, Berlin, Germany

³ DZHK (German Centre for Cardiovascular Research), partner site Berlin, 10115 Berlin, Germany

¹⁰ ⁴ Helmholtz Center Munich – German Research Center for Environmental Health, Institute of
¹¹ Computational Biology, Neuherberg, Munich, Germany

14 *authors contributed equally

15 **listed in alphabetical order

***correspondence: daniela.panakova@mdc-berlin.de, janphilipp.junker@mdc-berlin.de

17

18 Myocardial infarction is a leading cause of death worldwide, as the adult human heart
19 does not have the ability to regenerate efficiently after insults. In contrast, the adult
20 zebrafish heart has a high capacity for regeneration, and understanding the
21 mechanisms of regenerative processes in fish allows identification of novel
22 therapeutic strategies. While several pro-regenerative factors have been described,
23 the cell types orchestrating heart regeneration remain largely elusive. To overcome
24 this conceptual limitation, we dissected cell type diversity in the regenerating
25 zebrafish heart based on single cell transcriptomics and spatiotemporal analysis. We
26 discovered a dramatic induction of several pro-regenerative cell types with fibroblast
27 characteristics. To understand the cascade of events leading to heart regeneration,
28 we determined the origin of these cell types by high-throughput lineage tracing. We
29 found that pro-regenerative fibroblasts are derived from two separate sources, the
30 epicardium and the endocardium. Mechanistically, we identified Wnt signaling as a
31 key regulator of the endocardial regenerative response. In summary, our results
32 uncover specialized fibroblast cell types as major drivers of heart regeneration,
33 thereby opening up new possibilities to interfere with the regenerative capacity of the
34 vertebrate heart.

35

36 Heart injury in mammals typically leads to permanent scarring. The zebrafish heart,
37 however, regenerates efficiently after injury, making zebrafish the preeminent model system
38 for heart regeneration (1,2). After cryoinjury, which mimics aspects of myocardial infarction,
39 the injured zebrafish heart undergoes a transient period of fibrosis (3), during which the
40 damaged heart muscle regenerates via dedifferentiation and proliferation of cardiomyocytes
41 (4,5). Many pathways and factors involved in heart regeneration have been described
42 (6,7,8,9). However, which specific cell types orchestrate the process of heart regeneration
43 remains unclear.

44 Important molecular signals for zebrafish heart regeneration emanate from the epi-
45 and endocardium (3,7,10,11). Other cell types are also required for regeneration:
46 inflammation is an early response to cryoinjury, and depletion of macrophages leads to
47 delayed regeneration (12,13). Moreover, fibroblasts are activated upon injury, and ablation
48 of fibroblasts leads to reduced cardiomyocyte proliferation (14). All of this suggests that cell
49 types, potentially of a transient nature, residing in the regenerative niche may be important
50 cellular regulators of regeneration. Broadly acting pathways like Wnt tend to influence
51 abundance and expression profiles of multiple cell types in the regenerating heart in
52 potentially complex ways that are difficult to disentangle (15). A combination of single-cell
53 analysis and functional experiments is therefore necessary to understand the role of
54 signaling pathways in regeneration.

55 A number of recent single-cell RNA-sequencing (scRNA-seq) studies have
56 determined cell type diversity in the developing and adult heart (16), including large-scale
57 single-cell analysis of the healthy human heart (17,18) as well as cell type changes in the
58 mouse after myocardial infarction (19). Furthermore, a single-cell analysis of sorted
59 zebrafish cardiomyocytes revealed metabolic changes during the regeneration process (20).
60 However, to date no systematic analysis of cardiac cell types in a regeneration-competent
61 organism has been performed. Consequently, our knowledge of the cellular composition of
62 the regenerative niche and the underlying signaling interactions remains incomplete. Hence,
63 current definitions of „activated“ macrophages and fibroblasts rely heavily on transgenes,
64 may be affected by observation bias, and probably underestimate the complexity of transient
65 cell types involved in regeneration. Moreover, the developmental origin of transient cell
66 types, as well as the pathways that generate them, remain unresolved. However, this
67 information is crucial in order to understand the mechanisms underlying generation and
68 activation of pro-regenerative cell types.

69

70 **The cellular composition of the regenerating heart**

71 For systematic identification of cardiac cell types in the healthy and regenerating zebrafish
72 heart, we performed scRNA-seq of around 200,000 dissociated cells at different stages pre-
73 and post-injury (Fig. 1A). To limit experimental biases, we did not apply any sorting
74 procedure. In order to include information about the developmental origin of cells, we applied
75 a method for massively parallel lineage tracing based on CRISPR/Cas9 technology
76 (21,22,23). By injecting Cas9 and a sgRNA against a multi-copy transgene, we recorded
77 lineage relationships in early development by creating “genetic scars” that serve as lineage
78 barcodes (21).

79 We first assessed cell type diversity in the healthy and regenerating heart. Clustering
80 of single-cell transcriptomes revealed all major cardiac cell types (Fig. 1B, Fig. S1). As
81 expected, we observed a strong increase in fibroblasts and immune cells after injury (Fig.
82 1B). Closer inspection of the clustering data revealed a sub-structure among the cell types of
83 the three main layers of the heart – epicardium, myocardium and endocardium (Fig. S2). We
84 hypothesized that this cell type sub-structure might correspond to spatial differences due to
85 functional specification of these cell types in atrium and ventricle. By using the tomo-seq
86 method for spatially-resolved transcriptomics (24), and deconvolving this spatial data into
87 single-cell transcriptional profiles (25), we could validate atrial and ventricular enrichment for
88 some of these sub-cell-types (Fig. 1C). We confirmed this finding by physical separation of
89 the atrium and ventricle, followed by scRNA-seq (Fig. 1D).

90

91 **Identification of cellular drivers of heart regeneration**

92 We identified a further transcriptional sub-structure among the cardiomyocytes (Fig. 2A). In
93 addition to the normal adult cardiomyocytes, which are characterized e.g. by expression of
94 genes involved in ATP synthesis and the tricarboxylic acid cycle (*atp5pd*, *aldoaa*), we also
95 detected a smaller cluster characterized by genes related to cardiomyocyte development
96 (*ttn*, *bves*, *synpo2lb*). These dedifferentiated or newly formed cardiomyocytes, which are a
97 hallmark of the regenerating heart, increased in number already at 3 dpi (days post injury)
98 (Fig. 2A, Fig. S2).

99 We noticed that three well-established signaling factors in heart regeneration,
100 *aldh1a2* (6) (the enzyme producing retinoic acid), the cardiomyocyte mitogen *nrg1* (26), and
101 the pro-regenerative extra-cellular matrix (ECM) factor *fn1a* (27), are strongly enriched in
102 fibroblasts (Fig. 2B). This prompted us to investigate the diversity of cardiac fibroblasts in
103 more detail. Sub-clustering revealed an unexpectedly large cell type diversity with 13
104 transcriptionally distinct clusters of fibroblasts (Fig. 2C, Fig. S3), which exhibit pronounced
105 differences in their expression profiles of ECM related genes (Fig. 2D).

106 To focus our analysis on those fibroblast types that may be part of the regenerative
107 niche, we analyzed the dynamics of these cell types after injury. Three types of fibroblasts,
108 characterized by expression of *col11a1a*, *col12a1a*, and *nppc*, respectively, stood out as
109 being transiently present at the peak of regeneration (3 and 7 dpi) but virtually absent before
110 injury and after regeneration (Fig. 3A, Fig. S3). Interestingly, *col12a1a*, a non-fibrillar
111 collagen that may act as a matrix-bridging component, has already been shown to be
112 expressed in the epicardial and connective tissues upon heart injury (28) and is known to be
113 involved in regeneration of other organ systems in zebrafish (29). Two other cell types with
114 an ECM-related function, the perivascular cells as well as the valve fibroblasts, also
115 displayed upregulation after injury. Other fibroblast cell types displayed only moderate
116 changes after injury. Importantly, we noticed that established markers for “activated”
117 fibroblasts like *postnb* (14) captured some, but not all fibroblast types that are generated
118 upon injury, and were also expressed in non-fibroblast populations like the epicardial cells
119 (Fig. S4), suggesting that previous marker-based analysis underestimated the transcriptional
120 diversity of the cardiac fibroblast population.

121 To spatially resolve the response of all identified fibroblast cell types, we performed
122 fluorescent *in situ* hybridization (Fig. 3B, Fig. S5, S6). This analysis confirmed the location of
123 the transient fibroblast cell types in the injury area, further corroborating our hypothesis that
124 these cell types contribute to the regenerative niche and regulate injury response and/or
125 regeneration.

126 We next wanted to understand which of the transient fibroblast cell types express
127 signaling factors involved in heart regeneration (Fig. 3C, Fig. S7). We found particularly high
128 expression of *nrg1* in *col12a1a* fibroblasts, while *fn1a* is expressed almost exclusively in
129 *col11a1a* fibroblasts. Furthermore, we observed that retinoic acid (*aldh1a2*) is produced at
130 high levels by *nppc* fibroblasts as well as epicardium. Interestingly, we observed that the
131 retinoic acid readout gene *stra6* (30,31) is expressed highly and specifically in *col11/col12*
132 fibroblasts, but not in cardiomyocytes. Finally, we noticed a very specific interaction between
133 perivascular cells and blood vessel endothelium via *cxcl12b-cxcr4a* chemokine signaling.
134 Perivascular cells are a known regulator of blood-vessel formation (32), and it was recently
135 shown that *cxcl12b-cxcr4a* signaling is important for neovascularization of the regenerating
136 heart (33).

137 Finally, we reasoned that the *col11/col12* and *nppc* fibroblasts might express
138 additional secreted factors with a pro-regenerative function in heart regeneration. Indeed, a
139 bioinformatic analysis revealed that expression of secretome genes increases at 3 dpi and 7
140 dpi compared to uninjured control hearts (Fig. 3D, Fig. S8). Importantly, we found that the
141 *col11/col12* fibroblasts have the highest secretome expression of all detected cell types. The

142 secretome of *col11/col12* fibroblasts is enriched in genes with known functions in
143 regeneration, morphogenesis and tissue development (Fig. 3E, Fig. S8). Interestingly, the
144 secretome at 3 dpi is also enriched in genes with a function in angiogenesis (e.g. *angptl1a*
145 and *angptl2a*), suggesting a role of these cell types in neovascularization. We next
146 performed a ligand-receptor analysis for the identified cell types. We found that the number
147 of putative cell-cell interactions increased drastically after injury and peaked at 3 dpi (Fig.
148 S9), giving rise to a complex network of ingoing and outgoing connections with a noticeable
149 enrichment in fibroblast subtypes. Of note, we detected many incoming interactions for
150 *plvabp* blood vessel endothelial cells, indicating again a potential role of fibroblasts in
151 inducing neovascularization after heart injury..

152 In summary, based on their gene expression patterns, their timing of appearance,
153 and their spatial position in the injury area, we identified several fibroblast subtypes that
154 appear to be have a pro-regenerative function during heart regeneration: *col11/12*
155 fibroblasts, *nppc* fibroblasts, and perivascular cells.

156

157 **The origin of cardiac fibroblasts**

158 We next aimed to elucidate the origin of the transient pro-regenerative fibroblasts in order to
159 better understand their mechanism of activation. To analyze lineage relationships in a high-
160 throughput manner, we used the LINNAEUS method to reconstruct lineage trees for single
161 cells (21). In LINNAEUS, cells are marked by heritable DNA barcodes (genetic scars) in
162 reporter genes that are created by Cas9 during early development. The cell-specific
163 accumulation of these scars can then be used to determine lineage relationships between
164 the cells and build a lineage tree. Here, we injected Cas9 into 1-cell stage embryos in order
165 to record lineage relationships during early development, until gastrulation (21), that we read
166 out much later, in the adult heart (all lineage trees are shown in Fig. S10-13). By sequencing
167 scars and transcriptome from the same single cells, we can build lineage trees that reveal
168 shared developmental origins of cell types (Fig. 4A). In a lineage tree, all cells in a node
169 share the same developmental ancestor, and any transient cell originating from a cell in a
170 node would be found in the same node. We calculated correlations between cell type ratios
171 in the different tree nodes to determine which cell types are related by lineage (Fig. 4B).

172 Hierarchical clustering of these correlations revealed four clusters of cell types at 3
173 dpi, the earliest timepoint at which we detect the transient *col11a1a* and *col12a1a*
174 fibroblasts, and seven clusters at 7 dpi, the earliest timepoint at which we detect the
175 transient *nppc* fibroblasts (Fig. 4C, Fig. S14). At both timepoints all immune cells share a
176 common lineage, validating our approach. We observed a clustering of several fibroblast

177 types, including *col11a1a* and *col12a1a* fibroblasts, as well as constitutive fibroblasts,
178 together with the epicardial cells, strongly suggesting that these fibroblast cell types share a
179 developmental origin with the epicardium. Importantly, several fibroblast cell types (*nppc* and
180 *spock3* fibroblasts, valve fibroblasts) were not part of this cluster at 3 dpi and 7 dpi,
181 indicating that these fibroblasts may have a different origin (which we studied in more depth
182 later, in Fig. 4F, G). To validate the lineage origin of *col11a1a* and *col12a1a* fibroblasts, we
183 performed a genetic lineage tracing experiment based on Cre-Lox technology in
184 regenerating hearts using the transgenic line *Tg(tcf21:Cre^{ERT2}; ubi:Switch)*. Our scRNA-seq
185 data showed that *tcf21* is expressed in epicardial cells, constitutive fibroblasts and other
186 fibroblast types of the epicardial cluster (Fig. S15). After recombination, expression of
187 mCherry colocalizes with expression of *col12a1a* (Fig. 4D), corroborating the origin of the
188 transient *col11a1a* and *col12a1a* fibroblasts from either the epicardium or from epicardial-
189 derived fibroblasts.

190 LINNAEUS reliably identifies the developmental origin of cell types, but lineage
191 recording is limited to early development. It therefore remains unclear from which source cell
192 type the transient fibroblasts originate upon injury in the adult heart – for instance, we cannot
193 distinguish whether *col11a1a* and *col12a1a* fibroblasts are derived from epicardial cells,
194 constitutive fibroblasts, or any other cell type in the epicardial cluster. Furthermore,
195 expression of *tcf21* is not specific enough to address this question with our Cre-Lox lineage
196 tracing approach (Fig. S15). To further elucidate the origin of the transient fibroblast types,
197 we applied two transcriptome-based trajectory inference methods, partition-based graph
198 abstraction (34) (PAGA) and RNA velocity (35), to all cells from lineage-related clusters at 3
199 dpi (Fig. 4E) and 7 dpi (Fig. S16). Of note, when presented with all fibroblast cell types
200 without guidance from lineage trees, PAGA also connects cell types that are not related by
201 lineage according to LINNAEUS, such as *nppc* fibroblasts and epicardial fibroblasts (Fig.
202 S17). This suggests that for processes where several transcriptionally similar cell types are
203 created, integration with explicit lineage tracing methods such as LINNAEUS may be
204 necessary to distinguish real and spurious trajectories. Both timepoints (3 dpi and 7 dpi)
205 show that transient *col11a1a* and *col12a1a*-fibroblasts originate from the constitutive
206 fibroblasts, with an additional contribution from the epicardial cells at 7 dpi (Fig. 4F). Genes
207 that are upregulated along these trajectories are collagens *col11a1a* and *col12a1a*, the pro-
208 regenerative ECM factor *fn1a*, the epicardial activation marker *postnb*, the retinoic acid
209 signaling response gene *stra6*, and the cardiomyocyte mitogen *nrg1* (Fig. S16).

210 We next focused on the fibroblast types that do not belong to the cluster of
211 epicardium-derived cells, including the transient *nppc* fibroblasts (Fig. 2C). At 7 dpi, we
212 found that the different endocardial cell types (endocardium (Atrium), endocardium

213 (Ventricle) and endocardium (frzb) were present in over 80% of all nodes containing *nppc*
214 fibroblasts, suggesting a lineage relationship between this fibroblast type and the
215 endocardium (Fig. 4F). Similarly, endocardium (Ventricle) was present in over 80% of nodes
216 with *spock3* fibroblasts. A transcript trajectory analysis revealed transcriptional similarity and
217 a potential differentiation trajectory between *nppc* fibroblasts and the ventricular
218 endocardium (Fig. 4G), confirming their endocardial origin. We observed that *nppc*
219 fibroblasts continue to express endothelial genes (e.g. *vwf*, *fli1a*) in addition to ECM genes,
220 suggesting that they maintain at least parts of their endocardial gene expression after
221 turning on a fibrotic gene expression program.

222 Interestingly, the endocardial fibroblasts have low clonality, i.e. only a small fraction
223 of the nodes with endocardial cells also contains endocardial fibroblasts (Fig. S18),
224 suggesting that endocardial fibroblasts are only generated in a subset of the endocardium,
225 probably the injury area. We hypothesized that the internal position of the endocardium, as
226 well as the transient nature and low clonality of the *nppc* fibroblasts, means that these cells
227 are only generated upon an injury that is sufficiently deep to also damage the endocardium.
228 We confirmed that longer contact of the cryoprobe and the heart led to deeper injuries.
229 Indeed, longer exposure to the cryoprobe resulted in much stronger *nppc* expression beyond
230 the border zone, as opposed to injuries with shorter contact time (Fig. S18).

231 In summary, we combined massively parallel lineage tracing and trajectory inference
232 of single-cell transcriptomes in order to systematically identify the origin of cell types in the
233 regenerative niche. Our analyses revealed a clear separation of epicardial and endocardial-
234 derived fibroblasts, with both lineages giving rise to transient fibroblasts upon injury. While
235 the epicardial origin of cardiac fibroblasts has been clearly established in zebrafish, the
236 existence of atrial and ventricular fibroblasts of endocardial origin had previously not been
237 fully resolved (11,14). Given the endocardial origin of these cells, their expression of *aldh1a2*
238 (Fig. 3B), and their localization in the injury border zone (Fig. 3C), we conclude that the *nppc*
239 fibroblasts contribute significantly to retinoic acid signaling in the regenerative niche, which is
240 in line with the previously described endocardial contribution to retinoic acid signaling⁶.

241

242 **Cellular dissection of the role of canonical Wnt signaling**

243 While we established the pro-regenerative role of *col11*, *col12* and *nppc* fibroblasts based on
244 gene expression data, and identified their origin based on lineage analysis, it remains
245 unclear which signaling pathways are required to generate these transient fibroblast cell
246 types upon injury. Functional pathway inhibition experiments are required to determine
247 mechanisms of fibroblast activation. We noticed that fibroblasts express many genes related

248 to Wnt signaling (ligands, receptors, modulators) (Fig. 5A, Fig. S19), which inspired us to
249 investigate the role of canonical Wnt signaling in this system. The role of Wnt signaling in
250 heart regeneration remains an important open question (15): On the one hand, Wnt is
251 generally considered a pro-proliferative factor, and Wnt activation has been shown to be
252 beneficial for zebrafish fin and spinal cord regeneration (29),(36). On the other hand, it was
253 recently reported that activation of Wnt signaling suppressed cardiomyocyte proliferation
254 after ventricular apex resection (37). With our knowledge of cardiac cell types as well as
255 their origin, location and dynamics upon injury, we sought to dissect the potentially complex
256 effects of Wnt on the cellular level.

257 We therefore inhibited canonical Wnt signaling after cryoinjury by using the well-
258 characterized Wnt/β-catenin-dependent signaling inhibitor IWR-1 and observing its effects at
259 3, 7, 15, and 30 dpi (Fig. 5B). Wnt/β-catenin signaling inhibition led to a pronounced delay in
260 heart regeneration, with prolonged fibrosis and increased injury area compared to the control
261 (Fig. 5B), as previously reported (37). Single-cell transcriptomics of IWR-1-treated hearts at
262 3 dpi and 7 dpi revealed that cardiomyocyte dedifferentiation was delayed (Fig. 5C).
263 Compared to control samples, dedifferentiated cardiomyocytes were reduced at 3 dpi and
264 did not localize to the injury area at 7 dpi (Fig. 5C).

265 Intriguingly, the perivascular cells, as well as all endocardium-derived fibroblast types
266 (*nppc* fibroblasts, *spock3* fibroblasts, valve fibroblasts) were strongly reduced upon Wnt
267 inhibition, while all other fibroblast cell types were largely unaffected (Fig. 5D, Fig. S20). We
268 confirmed this finding by fluorescent *in situ* hybridization (Fig. 5E). This observation strongly
269 suggests that Wnt signaling is required for the activation of endocardial fibroblasts, akin to
270 the described role of Wnt in inducing endothelial-to-mesenchymal transition in mice (38,39).
271 We next examined the consequences of the depletion of perivascular cells. Based on high
272 expression of the chemokine *cxcl12b* in perivascular cells (Fig. 3B), we hypothesized this
273 cell type to be a major driver of neovascularization. Indeed, we observed that hypoxia
274 markers are upregulated in IWR-1 treated hearts upon injury (Fig. 5F), which may indicate a
275 tissue response to the loss of perivascular cells. In summary, we used inhibition of Wnt/β-
276 catenin signaling as a paradigm to dissect the function of complex signaling pathways on the
277 single-cell level. We discovered that Wnt/β-catenin signaling is essential for the transient
278 upregulation of endocardial-derived fibroblasts and perivascular cells, the consequences of
279 which are in agreement with the observed defects in cardiomyocytes response and impaired
280 regeneration.

281

282 **Discussion**

283 Here we used a sorting-free approach to determine the cellular composition of the
284 regenerative niche in the zebrafish heart based on single-cell transcriptomics as well as
285 spatio-temporal analysis. This allowed us to identify three transient cell types with fibroblast
286 characteristics (*col11/12* fibroblasts, *nppc* fibroblasts) that are major sources of known pro-
287 regenerative genes like *nrg1*, *fn1a* and retinoic acid and also express additional secreted
288 factors with a potential pro-regenerative function. These fibroblast cell types are ideally
289 suited as cellular drivers for regeneration based on their expression of pro-regenerative
290 factors, their location in the injury area, and their transient appearance after injury. By
291 combining high-throughput lineage tracing with RNA velocity and single-cell trajectory
292 inference, we were able to systematically identify the origin of these cell types. This
293 approach effectively combines information about two time points – CRISPR barcoding
294 during early development, and trajectory inference at the time of analysis – and can serve as
295 a blueprint for understanding the origin of transient cell types that are generated in disease
296 conditions. With this strategy we could classify cardiac fibroblasts into two groups, based on
297 their origin from either the epicardium or the endocardium. While the existence of epicardial
298 fibroblasts is firmly established, we now show that there are three types of endocardial
299 fibroblasts (*nppc* fibroblasts, *spock3* fibroblasts, valve fibroblasts). As an example for the
300 type of high-resolution cellular and molecular dissection of regulatory interactions that
301 becomes possible with our data, we performed an analysis of the effects of a broad
302 perturbation, Wnt inhibition, which revealed that Wnt is required for activation of all
303 endocardial fibroblasts.

304 Among the three types of endocardial fibroblasts, the *nppc* fibroblasts are unique
305 because they are completely absent in the healthy heart and are generated in the injury area
306 only upon deep injury directly affecting the endocardium. The epicardium-derived transient
307 *col11/12* fibroblasts are the cell type that corresponds most closely to the “activated”
308 fibroblasts previously described in the literature (14). Interestingly, they appear to be induced
309 via retinoic acid, which is produced in a variety of cell types, including the epicardium and
310 *nppc* fibroblasts. Hence, the described pro-regenerative function of retinoic acid is at least
311 partially indirect, acting via induction of *col11/col12* fibroblasts, which in turn produce pro-
312 regenerative factors. The perivascular cells are another interesting cell type with fibroblast
313 characteristics: In contrast to previous reports, our data shows that the perivascular cells are
314 not the only source of *nrg1* (26), but we found that they are the source of *cxcl12b*, a major
315 factor in revascularization after heart injury, whose source had previously not been reported
316 (33). In summary, our detailed cellular dissection of the fibrotic response in the zebrafish
317 heart shows previously unknown sources and mechanisms of pro-regenerative programs.

318 This large diversity of different fibroblast cell populations challenges the concept of
319 the fibroblast as a well-defined cell type, and suggests that fibrosis should be seen as a
320 collective phenomenon to which a variety of cell types contribute. We here focused our
321 analysis on cell types that have a clear pro-regenerative function based on their expression
322 profile. Understanding the role of cell types with a less obvious function in heart
323 regeneration, including other fibroblast populations or immune cell types, requires targeted
324 cell type depletion experiments (40), which can be set up using our atlas. Only relatively few
325 factors with a clear pro-regenerative function in heart regeneration have been discovered
326 (2). It is likely that the transient cell types we identified express additional pro-regenerative
327 genes, and our list of differentially expressed secreted factors is a powerful resource for
328 identification of those factors.

329 The zebrafish heart is highly similar to the human heart, and the pathways that
330 contribute to the regenerative capacity of the zebrafish heart are conserved. Thus, our
331 analysis may lead us to better understand the limited regenerative capacity of the human
332 heart, and it opens up an exciting strategy to identify novel therapeutic approaches. Our
333 dataset, as well as the experimental and computational approaches presented here, will
334 serve as a powerful resource for identification of candidate interactions between cell types
335 involved in heart regeneration.

336

337 **Author contributions**

338 B.H., S.L., B.S., D.P. and J.P.J. conceived and designed the project. B.H. performed single-
339 cell experiments and mRNA and cell type analysis, with support by B.S.. S.L. and M.G.S. did
340 cryoinjury experiments. S.L. performed and analyzed histology, RNAscope, CreLox lineage
341 tracing and Wnt inhibition experiments. B.S. built single-cell lineage trees, developed tree
342 analysis methods, and performed trajectory and RNA velocity analysis. H.A. adapted bulk
343 deconvolution to tomo-seq data, with guidance from B.S. and F.T.. D.P. and J.P.J. guided
344 experiments, and J.P.J. guided data analysis. B.H., B.S. and J.P.J. wrote the manuscript, in
345 close interaction with S.L. and D.P., and with input from all other authors. All authors
346 discussed and interpreted results.

347

348 **Acknowledgements**

349 We acknowledge support by MDC/BIMSB core facilities (zebrafish, light microscopy,
350 genomics, bioinformatics), and we thank J. Richter for help with zebrafish experiments. Work
351 in D.P.'s laboratory was supported by the DZHK (German Centre for Cardiovascular

352 Research) and by the BMBF (German Ministry of Education and Research). Work in J.P.J.'s
353 laboratory was funded by a European Research Council Starting Grant (ERC-StG 715361
354 SPACEVAR), a Fondation Leducq Transatlantic Networks Grant (16CVD03), and a
355 Helmholtz Incubator grant (Sparse2Big ZT-I-0007). B.H. was supported by a PhD fellowship
356 from Studienstiftung des deutschen Volkes.

357

358

359 **References**

- 360 1. K. D. Poss, Heart Regeneration in Zebrafish. *Science*. **298**, 2188–2190 (2002).
- 361 2. J. M. Gonzalez-Rosa, C. E. Burns, C. G. Burns, Zebrafish heart regeneration: 15 years of
362 discoveries. *Regeneration*. **4**, 105–123 (2017).
- 363 3. J. M. Gonzalez-Rosa, V. Martin, M. Peralta, M. Torres, N. Mercader, Extensive scar
364 formation and regression during heart regeneration after cryoinjury in zebrafish.
365 *Development*. **138**, 1663–1674 (2011).
- 366 4. K. Kikuchi, J. E. Holdway, A. A. Werdich, R. M. Anderson, Y. Fang, G. F. Egnaczyk, T.
367 Evans, C. A. MacRae, D. Y. R. Stainier, K. D. Poss, Primary contribution to zebrafish
368 heart regeneration by gata4+ cardiomyocytes. *Nature*. **464**, 601–605 (2010).
- 369 5. C. Jopling, E. Sleep, M. Raya, M. Martí, A. Raya, J. C. I. Belmonte, Zebrafish heart
370 regeneration occurs by cardiomyocyte dedifferentiation and proliferation. *Nature*. **464**,
371 606–609 (2010).
- 372 6. K. Kikuchi, J. E. Holdway, R. J. Major, N. Blum, R. D. Dahn, G. Begemann, K. D. Poss,
373 Retinoic Acid Production by Endocardium and Epicardium Is an Injury Response
374 Essential for Zebrafish Heart Regeneration. *Developmental Cell*. **20**, 397–404 (2011).
- 375 7. Y. Fang, V. Gupta, R. Karra, J. E. Holdway, K. Kikuchi, K. D. Poss, Translational profiling
376 of cardiomyocytes identifies an early Jak1/Stat3 injury response required for zebrafish
377 heart regeneration. *Proceedings of the National Academy of Sciences*. **110**, 13416–
378 13421 (2013).
- 379 8. Y. Han, A. Chen, K.-B. Umansky, K. A. Oonk, W.-Y. Choi, A. L. Dickson, J. Ou, V.
380 Cigliola, O. Yifa, J. Cao, V. A. Tornini, B. D. Cox, E. Tzahor, K. D. Poss, Vitamin D
381 Stimulates Cardiomyocyte Proliferation and Controls Organ Size and Regeneration in
382 Zebrafish. *Developmental Cell*. **48**, 853–863.e5 (2019).
- 383 9. C.-C. Wu, F. Kruse, M. D. Vasudevarao, J. P. Junker, D. C. Zebrowski, K. Fischer, E. S.
384 Noël, D. Grün, E. Berezikov, F. B. Engel, A. van Oudenaarden, G. Weidinger, J.
385 Bakkers, Spatially Resolved Genome-wide Transcriptional Profiling Identifies BMP
386 Signaling as Essential Regulator of Zebrafish Cardiomyocyte Regeneration.
387 *Developmental Cell*. **36**, 36–49 (2016).
- 388 10. A. Lepilina, A. N. Coon, K. Kikuchi, J. E. Holdway, R. W. Roberts, C. G. Burns, K. D.
389 Poss, A Dynamic Epicardial Injury Response Supports Progenitor Cell Activity during
390 Zebrafish Heart Regeneration. *Cell*. **127**, 607–619 (2006).

391 11. J. Münch, D. Grivas, Á. González-Rajal, R. Torregrosa-Carrión, J. L. de la Pompa,
392 Notch signalling restricts inflammation and *serpine1* expression in the dynamic
393 endocardium of the regenerating zebrafish heart. *Development*. **144**, 1425–1440
394 (2017).

395 12. A.-S. de Preux Charles, T. Bise, F. Baier, J. Marro, A. Jaźwińska, Distinct effects of
396 inflammation on preconditioning and regeneration of the adult zebrafish heart. *Open
397 Biol.* **6**, 160102 (2016).

398 13. S.-L. Lai, R. Marín-Juez, P. L. Moura, C. Kuenne, J. K. H. Lai, A. T. Tsedeke, S.
399 Guenther, M. Looso, D. Y. Stainier, Reciprocal analyses in zebrafish and medaka
400 reveal that harnessing the immune response promotes cardiac regeneration. *eLife*. **6**,
401 e25605 (2017).

402 14. H. Sánchez-Iranzo, M. Galardi-Castilla, A. Sanz-Morejón, J. M. González-Rosa, R.
403 Costa, A. Ernst, J. Sainz de Aja, X. Langa, N. Mercader, Transient fibrosis resolves via
404 fibroblast inactivation in the regenerating zebrafish heart. *Proc Natl Acad Sci USA*. **115**,
405 4188–4193 (2018).

406 15. G. Ozhan, G. Weidinger, *Cell Regeneration* (2015), doi:10.1186/s13619-015-0017-8.

407 16. D. T. Paik, S. Cho, L. Tian, H. Y. Chang, J. C. Wu, Single-cell RNA sequencing in
408 cardiovascular development, disease and medicine. *Nat Rev Cardiol* (2020),
409 doi:10.1038/s41569-020-0359-y.

410 17. N. R. Tucker, M. Chaffin, S. J. Fleming, A. W. Hall, V. A. Parsons, K. C. Bedi Jr, A.-D.
411 Akkad, C. N. Herndon, A. Arduini, I. Papangeli, C. Roselli, F. Aguet, S. H. Choi, K. G.
412 Ardlie, M. Babadi, K. B. Margulies, C. M. Stegmann, P. T. Ellinor, *Circulation* (2020),
413 doi:10.1161/CIRCULATIONAHA.119.045401.

414 18. M. Litviňuková, C. Talavera-López, H. Maatz, D. Reichart, C. L. Worth, E. L. Lindberg,
415 M. Kanda, K. Polanski, M. Heinig, M. Lee, E. R. Nadelmann, K. Roberts, L. Tuck, E. S.
416 Fasouli, D. M. DeLaughter, B. McDonough, H. Wakimoto, J. M. Gorham, S. Samari, K.
417 T. Mahbubani, K. Saeb-Parsy, G. Patone, J. J. Boyle, H. Zhang, H. Zhang, A. Viveiros,
418 G. Y. Oudit, O. Bayraktar, J. G. Seidman, C. E. Seidman, M. Noseda, N. Hubner, S. A.
419 Teichmann, Cells of the adult human heart. *Nature* (2020), doi:10.1038/s41586-020-
420 2797-4.

421 19. N. Farbehi, R. Patrick, A. Dorison, M. Xaymardan, V. Janbandhu, K. Wystub-Lis, J. W.
422 Ho, R. E. Nordon, R. P. Harvey, Single-cell expression profiling reveals dynamic flux of
423 cardiac stromal, vascular and immune cells in health and injury. *eLife*. **8**, e43882
424 (2019).

425 20. H. Honkoop, D. E. de Bakker, A. Aharonov, F. Kruse, A. Shakked, P. D. Nguyen, C. de
426 Heus, L. Garric, M. J. Muraro, A. Shoffner, F. Tessadori, J. C. Peterson, W. Noort, A.
427 Bertozzi, G. Weidinger, G. Posthuma, D. Grün, W. J. van der Laarse, J. Klumperman,
428 R. T. Jaspers, K. D. Poss, A. van Oudenaarden, E. Tzahor, J. Bakkers, Single-cell
429 analysis uncovers that metabolic reprogramming by ErbB2 signaling is essential for
430 cardiomyocyte proliferation in the regenerating heart. *eLife*. **8**, e50163 (2019).

431 21. B. Spanjaard, B. Hu, N. Mitic, P. Olivares-Chauvet, S. Janjuha, N. Ninov, J. P. Junker,
432 Simultaneous lineage tracing and cell-type identification using CRISPR-Cas9-induced
433 genetic scars. *Nature Biotech.* **36**, 469–473 (2018).

434 22. B. Raj, D. E. Wagner, A. McKenna, S. Pandey, A. M. Klein, J. Shendure, J. A. Gagnon,
435 A. F. Schier, Simultaneous single-cell profiling of lineages and cell types in the
436 vertebrate brain. *Nature Biotech.* **36**, 442–450 (2018).

437 23. A. Alemany, M. Florescu, C. S. Baron, J. Peterson-Maduro, A. van Oudenaarden,
438 Whole-organism clone tracing using single-cell sequencing. *Nature*. **556**, 1–22 (2018).

439 24. J. P. Junker, E. S. Noël, V. Guryev, K. A. Peterson, G. Shah, J. Huisken, A. P.
440 McMahon, E. Berezikov, J. Bakkers, A. van Oudenaarden, Genome-wide RNA
441 Tomography in the Zebrafish Embryo. *Cell*. **159**, 662–675 (2014).

442 25. H. Aliee, F. Theis, “AutoGeneS: Automatic gene selection using multi-objective
443 optimization for RNA-seq deconvolution” (preprint, Bioinformatics, 2020), ,
444 doi:10.1101/2020.02.21.940650.

445 26. M. Gemberling, R. Karra, A. L. Dickson, K. D. Poss, Nrg1 is an injury-induced
446 cardiomyocyte mitogen for the endogenous heart regeneration program in zebrafish.
447 *eLife*. **4**, e05871 (2015).

448 27. J. Wang, R. Karra, A. L. Dickson, K. D. Poss, Fibronectin is deposited by injury-
449 activated epicardial cells and is necessary for zebrafish heart regeneration.
450 *Developmental Biology*. **382**, 427–435 (2013).

451 28. J. Marro, C. Pfefferli, A.-S. de Preux Charles, T. Bise, A. Jaźwińska, Collagen XII
452 Contributes to Epicardial and Connective Tissues in the Zebrafish Heart during
453 Ontogenesis and Regeneration. *PLoS ONE*. **11**, e0165497 (2016).

454 29. D. Wehner, T. M. Tsarouchas, A. Michael, C. Haase, G. Weidinger, M. M. Reimer, T.
455 Becker, C. G. Becker, Wnt signaling controls pro-regenerative Collagen XII in functional
456 spinal cord regeneration in zebrafish. *Nat Commun.* **8**, 126 (2017).

457 30. P. Bouillet, M. Oulad-Abdelghani, S. Vicaire, J.-M. Garnier, B. Schuhbaur, P. Dollé, P.
458 Chambon, Efficient Cloning of cDNAs of Retinoic Acid-Responsive Genes in P19
459 Embryonal Carcinoma Cells and Characterization of a Novel Mouse Gene, Stra1
460 (Mouse LERK-2/Eplg2). *Developmental Biology*. **170**, 420–433 (1995).

461 31. A. Isken, M. Golczak, V. Oberhauser, S. Hunzelmann, W. Driever, Y. Imanishi, K.
462 Palczewski, J. von Lintig, RBP4 Disrupts Vitamin A Uptake Homeostasis in a STRA6-
463 Deficient Animal Model for Matthew-Wood Syndrome. *Cell Metabolism*. **7**, 258–268
464 (2008).

465 32. G. Bergers, S. Song, The role of pericytes in blood-vessel formation and maintenance.
466 *Neuro-Oncology*. **7**, 452–464 (2005).

467 33. R. Marín-Juez, H. El-Sammak, C. S. M. Helker, A. Kamezaki, S. T. Mullapuli, S.-I. Bibi,
468 M. J. Foglia, I. Fleming, K. D. Poss, D. Y. R. Stainier, Coronary Revascularization
469 During Heart Regeneration Is Regulated by Epicardial and Endocardial Cues and
470 Forms a Scaffold for Cardiomyocyte Repopulation. *Developmental Cell*. **51**, 503-515.e4
471 (2019).

472 34. F. A. Wolf, F. K. Hamey, M. Plass, J. Solana, J. S. Dahlin, B. Göttgens, N. Rajewsky, L.
473 Simon, F. J. Theis, PAGA: graph abstraction reconciles clustering with trajectory
474 inference through a topology preserving map of single cells. *Genome Biology*. **20**, 59
475 (2019).

476 35. G. La Manno, R. Soldatov, A. Zeisel, E. Braun, H. Hochgerner, V. Petukhov, K.
477 Lidschreiber, M. E. Kastriti, P. Lönnerberg, A. Furlan, J. Fan, L. E. Borm, Z. Liu, D.
478 Bruggen, J. Guo, X. He, R. Barker, E. Sundström, G. Castelo-Branco, P. Cramer, I.
479 Adameyko, S. Linnarsson, P. V. Kharchenko, RNA velocity of single cells. *Nature*. **560**,
480 1–25 (2018).

481 36. B. Chen, M. E. Dodge, W. Tang, J. Lu, Z. Ma, C.-W. Fan, S. Wei, W. Hao, J. Kilgore, N.
482 S. Williams, M. G. Roth, J. F. Amatruda, C. Chen, L. Lum, Small molecule–mediated
483 disruption of Wnt-dependent signaling in tissue regeneration and cancer. *Nat Chem
484 Biol.* **5**, 100–107 (2009).

485 37. L. Zhao, R. Ben-Yair, C. E. Burns, C. G. Burns, Endocardial Notch Signaling Promotes
486 Cardiomyocyte Proliferation in the Regenerating Zebrafish Heart through Wnt Pathway
487 Antagonism. *Cell Reports*. **26**, 546–554.e5 (2019).

488 38. O. Aisagbonhi, M. Rai, S. Ryzhov, N. Atria, I. Feoktistov, A. K. Hatzopoulos,
489 Experimental myocardial infarction triggers canonical Wnt signaling and endothelial-to-
490 mesenchymal transition. *Disease Models & Mechanisms*. **4**, 469–483 (2011).

491 39. J. Duan, C. Gherghe, D. Liu, E. Hamlett, L. Srikantha, L. Rodgers, J. N. Regan, M.
492 Rojas, M. Willis, A. Leask, M. Majesky, A. Deb, Wnt1/βcatenin injury response
493 activates the epicardium and cardiac fibroblasts to promote cardiac repair:
494 Wnt1/βcatenin injury response regulates cardiac repair. *The EMBO Journal*. **31**, 429–
495 442 (2012).

496 40. J. R. Mathias, Z. Zhang, M. T. Saxena, J. S. Mumm, Enhanced Cell-Specific Ablation in
497 Zebrafish Using a Triple Mutant of Escherichia ColiNitroreductase. *Zebrafish*. **11**, 85–
498 97 (2014).

499

500

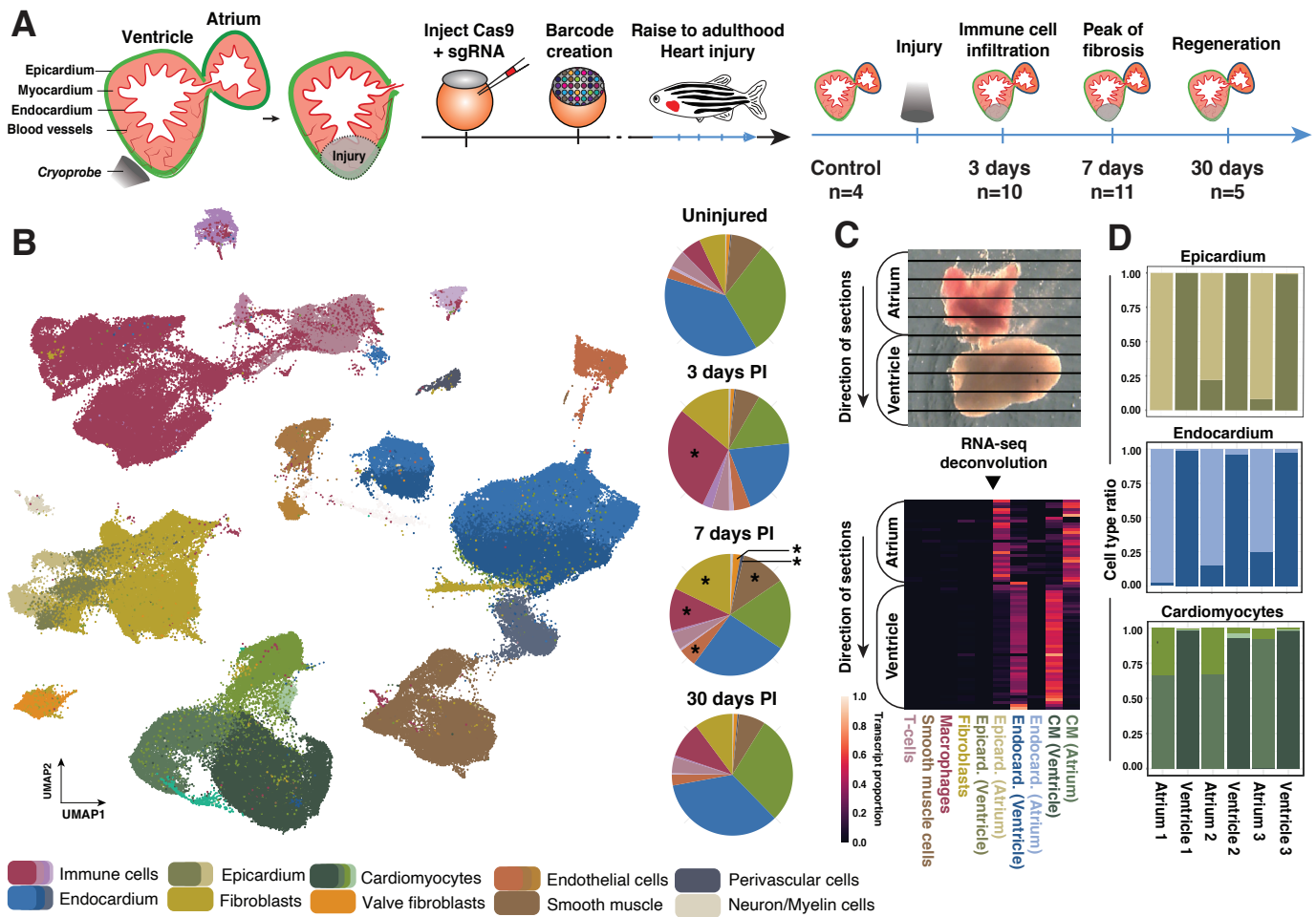


Figure 1. The cellular composition of the regenerating heart. (A) Cartoon of the experimental approach. Cells are barcoded during early development, and fish are raised to adulthood. Hearts were harvested either as an uninjured control or at 3, 7 or 30 days post injury (dpi). **(B)** UMAP representation of single-cell RNA-seq data and clustering results. Pie charts show the proportions of different cell types at different time points after injury. In the pie chart representation, similar cell types are grouped and shown by one (representative) color. Asterics (*) denote cell types with a statistically significant change in proportions compared to uninjured control. **(C)** Mapping of single cell data onto a spatially-resolved tomo-seq dataset. A computational deconvolution approach reveals chamber-specific sub-cell-types. **(D)** Distribution of subtypes of cardiomyocytes, endocardial cells, and epicardial cells for scRNA-seq datasets in which atrium and ventricle were physically separated. Color scheme as in Fig. S2.

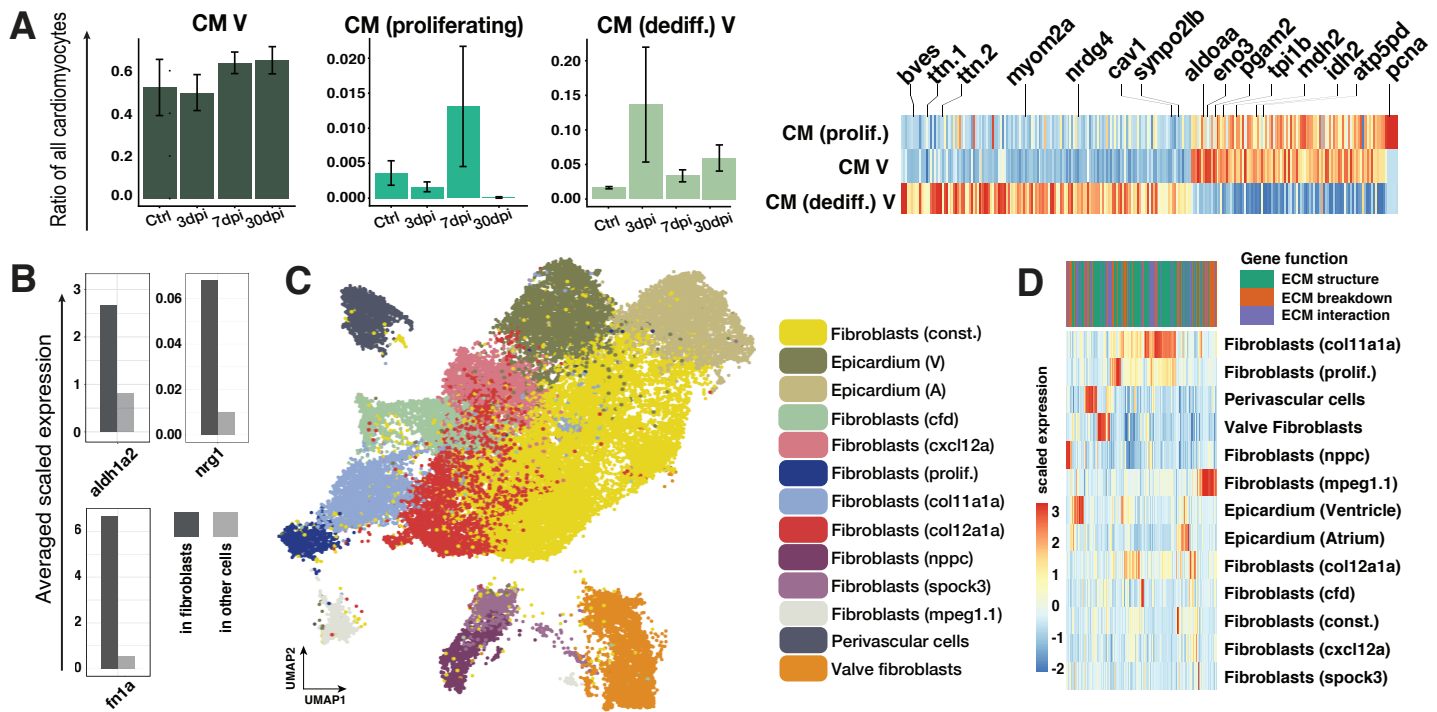
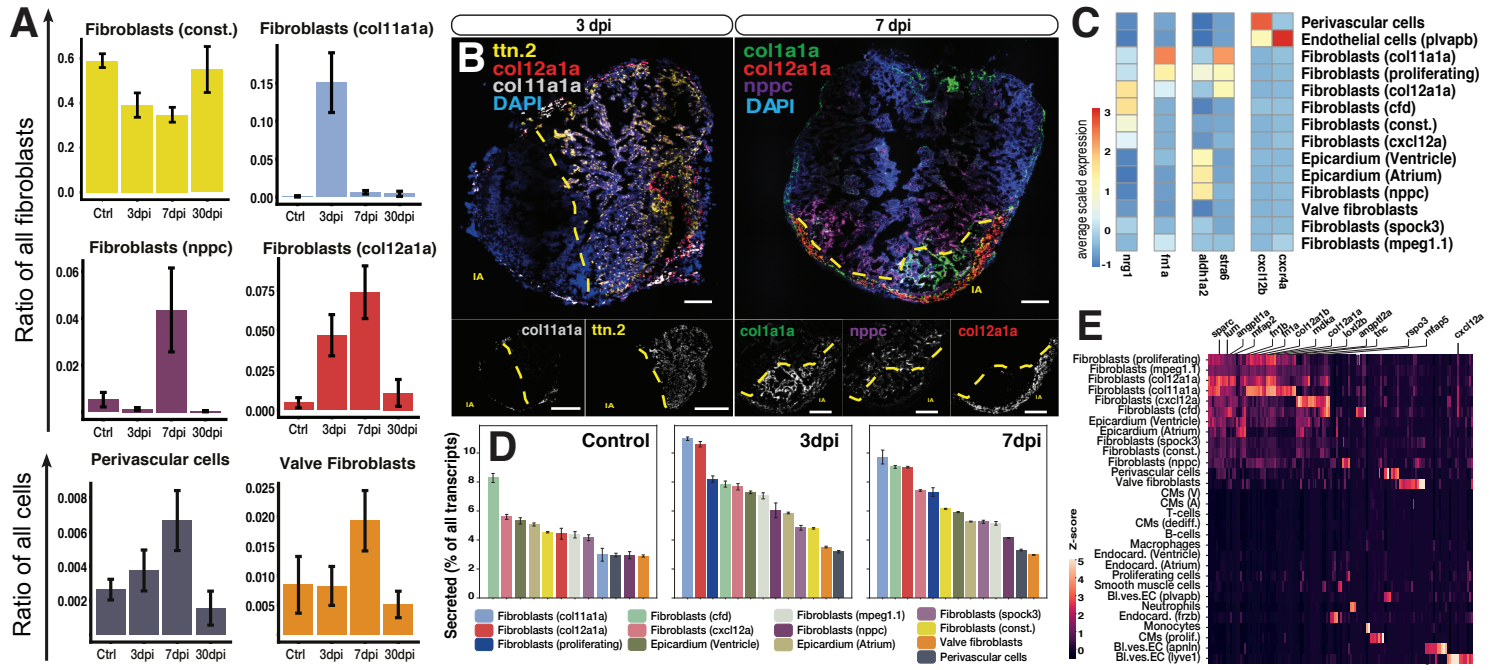


Figure 2. Cell type diversity of cardiac fibroblasts.

different subtypes of cardiomyocytes (CM) across the timepoints (error bars show standard error of the mean). Right: Differentially expressed genes between subtypes of cardiomyocytes. **(B)** Comparison of average expression of known pro-regenerative factors in fibroblasts and other cell types. **(C)** UMAP representation of subclustering of col1a1a expressing cells. **(D)** Expression of extracellular matrix (ECM) related genes in different fibroblast cell types. The genes are classified according to their contribution to structure, breakdown or interaction of the ECM.

(A) Left: Relative changes of abundance for

different cell types. Right: Heatmap showing scaled expression of ECM related genes across various fibroblast cell types.



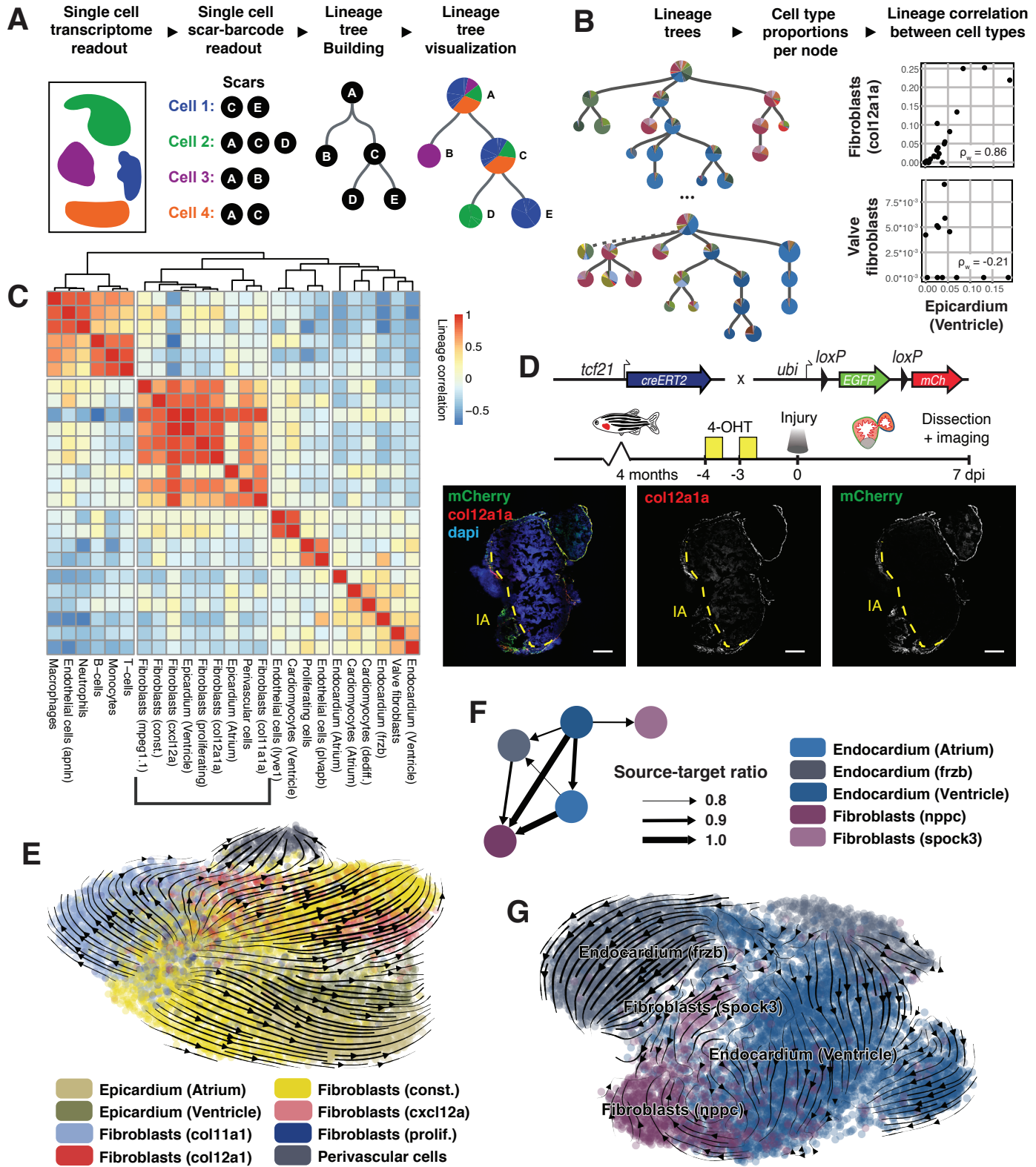


Figure 4. The origin of cardiac fibroblasts. **(A)** Cartoon of lineage tree construction using LINNAEUS. **(B)** We calculate weighted correlations of cell types over the trees in order to quantify lineage similarity. **(C)** Clustering by lineage correlations at 3 dpi reveals epicardial origin of many niche fibroblasts. **(D)** Microscopy-based lineage tracing confirms epicardial/fibroblast origin of col12a1a fibroblasts. **(E)** Trajectory analysis suggest constitutive fibroblasts as the source of col11a1a and col12a1a fibroblasts at 3 dpi. **(F)** Nppc fibroblasts share asymmetric lineage similarities with endocardial cell types at 7 dpi. **(G)** Trajectory analysis indicates transitions from endocardial cells to spock3 and nppc fibroblasts. Scale bar: 100 μ m.

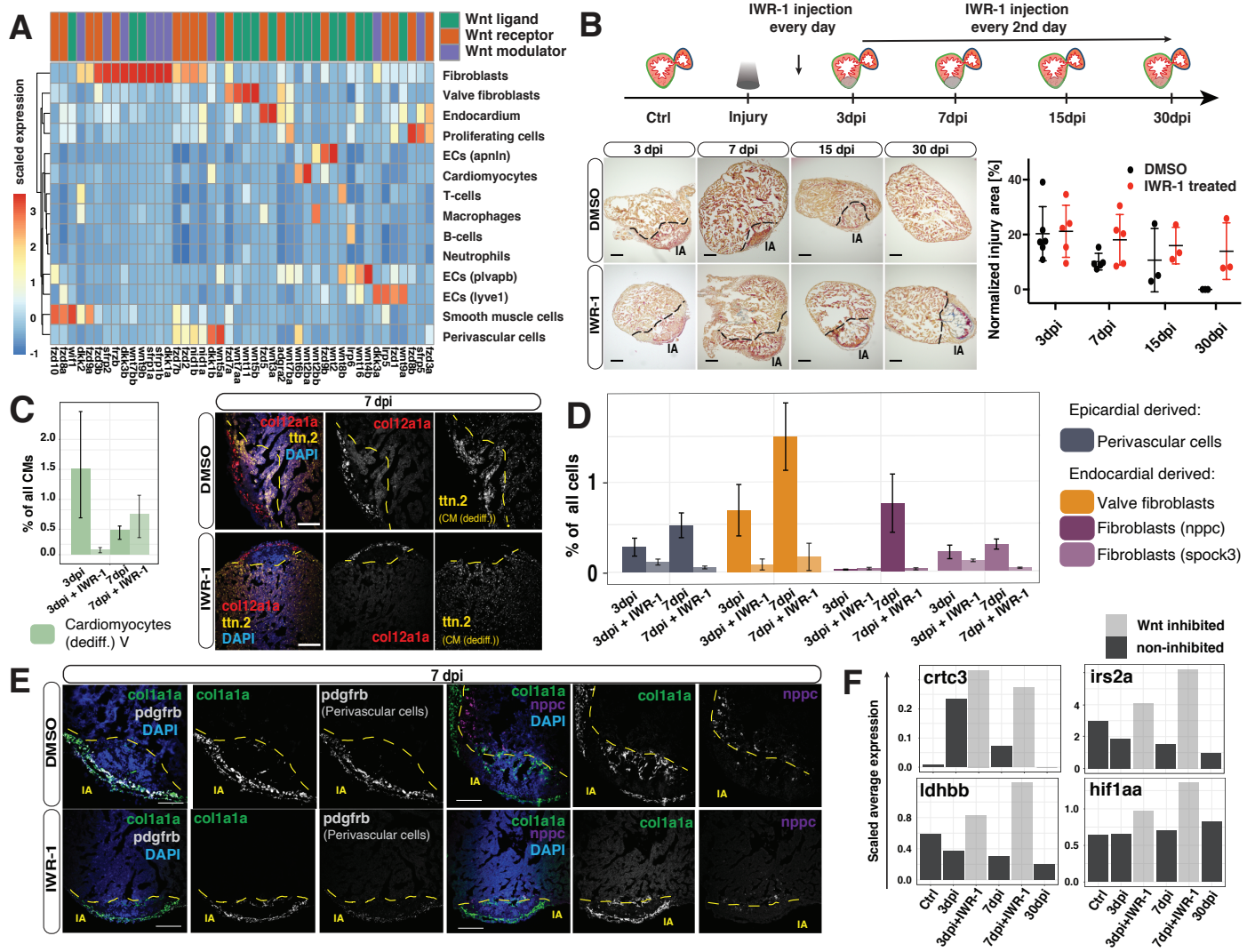


Figure 5. Cellular dissection of the role of canonical Wnt signaling. (A) Expression of Wnt signaling factors in the different cell types of the zebrafish heart. (B) Upper panel: Cartoon summary of IWR-1 Wnt inhibition experiments. Lower left: Histological comparison of the injury area (IA) at different time points after injury with or without Wnt inhibition. Scale bar: 300 μ m. Lower right: Relative size of the injury area across all histological replicates, mean and standard deviation are shown. (C) Left: Changes in number of dedifferentiated cardiomyocytes at 3 and 7 dpi between Wnt inhibited and control hearts. Right: Localization of dedifferentiated (tttn.2) cardiomyocytes at 7 dpi in the injured heart with or without Wnt inhibitor. (D) Changes in abundance of non-cardiomyocyte cell types upon Wnt inhibition at 3 and 7 dpi. (in (C) and (D), error bars show standard error of the mean) (E) Fluorescent in-situ hybridization of perivascular cells (white) and fibroblasts (nppc) (purple) in injured hearts at 7 dpi with or without Wnt inhibition. (in (C) and (E), scale bar: 100 μ m) (F) Expression of hypoxia induced genes at 3 and 7 dpi with and without Wnt inhibition.